Fatigue-life prediction methods of a dynamic power cable for a floating testing platform – a numerical approach

Daniela Benites-Munoz, Pierpaolo Ricci, Imanol Touzon, Fernando Salcedo, Rupert Raymond, and Diogo Nunes

Abstract—**Power cables are often used to connect marine systems to subsea electric grids. These cables are commonly exposed to the cyclic loads resulting from the waves, current and the floater's motions. Hence, the fatigue life plays a crucial role in the design stage of the behaviour and integrity of power cables. This paper addresses the fatigue-based design of a dynamic power cable deployed to connect a floating testing platform, HarshLab 2.0. Different fatigue-life prediction methods are examined, considering the damage in the steel armour and the conductor cores of the cable. The study is undertaken by estimating each cable component's long-term cyclic loading and comparing it with its resistance to fatigue damage. In this case, the damage for each variable was derived from $\sigma - N$ and $\epsilon - N$ curves, depending on the selected approach. The design iterative process led to the definition of a Lazy Wave design with a high-level optimisation of some components, e.g., the ballast and buoyancy modules and the bend stiffener. Generally, the behaviour across the cable length is similar between the different fatigue-life approaches, with the most significant expected fatigue damage found in localised hot spots near the bend stiffener and the belly (sag-bend region) of the cable. It is found that, despite a significant difference across the magnitude of fatigue life estimated in sensitive areas, the proposed layout complies with the fatigue life design criteria.**

Index Terms—**Dynamic power cable, Fatigue-life prediction, Numerical modelling, OrcaFlex**

I. Introduction

FLOATING testing platforms and marine energy devices use Dynamic Power Cables (DPC) to connect to the testing centres or the national grids. These power cables are an inherent component in the reliable operation of the floating system, and ensuring their integrity throughout the project's design life is sought from the early stages of the design. Common failures for DPC are associated with fatigue damage and their response in survivability conditions [1]. While the former is related to the normal operating loads affecting the performance of the DPC, the latter is characterised by the DPC withstanding extreme on-site sea conditions (single occurrences of the loads).

Dynamic power cables are built by a set of conductors. Primarily, these conductors are made of several wires that can be of copper or aluminium. Additionally, an armour steel layer is often employed for structural support and protection [2]. When designing the subsea cable layout, bend stiffeners are installed to endure the dynamic loads acting on the cable [3]. Moreover, to minimise the DPC response to cyclic loads, the layout is complemented with ancillary such as buoyancy and ballast modules.

It is expected that during the operation of the floating platform, the power cable will be subjected to cyclic loads caused by the waves, the current and the buoy motion. These loads induce a variation in the tension and the torque, whereas an alteration in the cable curvature contributes to the bending loads.

A common approach to understanding these cyclic loads and the limit of a mechanical component is the *S-N* curves, which describe the number of cycles, *N*, that lead to fatigue failure of the different components of a system under oscillating loads identified by the stress range, *S*.

In principle, high-cycle loading region is associated with the calculation of elastic stress due to the lowest stresses in the S-N curve. In contrast, for the highest stresses, the low-cycle loading region is related to the calculation of strain (including plastic response), [4]. For the latter, this is applicable when considering materials that may be deformed non-linearly, such as copper. Hence, accurately estimating the fatigue life of these cables has proved challenging due to their material, arrangement, and geometric nonlinearities [5]. This estimation leads to recommendations regarding the cable specifications and its subsea layout.

This paper addresses the estimation of the fatigue life of the DPC connecting a floating testing platform, HarshLab 2.0, to the Biscay Marine Energy Platform (BiMEP). As part of the design stage, the subsea cable layout and its components were evaluated by modelling different configurations. Different approaches to estimate the fatigue life were further investigated to meet the criteria conditions by using a method representing the system and its operating conditions. The most occurring conditions at the operation site are

D. Benites-Munoz, R. Raymond, and D. Nunes are with Tadek Limited, One Crown Square, Church Street East, Woking, GU21 6HR, United Kingdom. (e-mail: daniela.benites@tadek.co.uk, rupert.raymond@tadek.co.uk, and diogo.nunes@tadek.co.uk).

P. Ricci was with Tadek Limited. He is now at SSE Renewables, 1 Forbury Place, Forbury Road, Reading, RG1 3JH. (e-mail: pierpaolo.ricci@sse.com).

I. Touzon, and F. Salcedo are with Tecnalia, Parque Científico y Tecnológico de Bizkaia, Astondo Bidea, Edificio 700, E-48160 Derio (Bizkaia), Spain. (e-mail: imanol.touzon@tecnalia.com, and fernando.salcedo@tecnalia.com).

Digital Object Identifier:
https://doi.org/10.36688/ewtec-2023-410

Fig. 1. HarshLab 2.0 operating at BiMEP, retrieved from [6].

considered for the fatigue analyses undertaken.

II. Case study: floating platform

Tecnalia has developed a floating testing platform for materials, subsystems and components named HarshLab 2.0 (HL2.0); see Fig. 1. The platform can provide demonstration facilities for various technologies, materials, and coatings in extreme marine conditions. The modular design was deployed to a pre-installed mooring system in Berth 1 at the BiMEP test, where the HarshLab 1.0 was located. Furthermore, the HL2.0 will be connected to the grid by a dynamic electric cable to feed power to the equipment onboard for testing and monitoring.

A. Water depth and tidal range

The water depth at the position of HL2.0 is approximately 60 m LAT (Lowest Astronomical Tide), with an average gradient sloping offshore. Despite the extreme sea level measured at the site is ±3 m, the water depth is set to the MSL (Mean Sea Level) for the fatigue analysis to average the daily tidal variation of the water column height.

B. Environmental conditions

Waves at the BiMEP are characterised by a relatively wide range of periods, with extreme waves occasionally associated with high steepness and short periods, despite the influence of long swells from the Atlantic Ocean [7].

The load cases for this study were generated based on the field data from the BiMEP metocean analysis report [7]. The significant wave height and peak periods considered were extracted from the annual wave height and peak period probabilities, filtering for waves with an occurrence greater than 0.5%. By applying a 0.5% threshold, the number of computational simulations for the fatigue-life estimations results in a total of 51 sea states. The sea states with 0.5% probability of occurrence or more cover more than 92% of the potential occurrences at the BiMEP.

Due to the limited directionality of waves at the mooring site, only one wave direction was selected

Hs [m] (top of the bin) \ Tp [s] (top of the bin)	3	4	5	6	7	8	9	10	11	12	14	17	>17	Total
>6														0.0%
6														0.0%
5.5														0.0%
5														0.0%
4.5												0.6%		0.6%
4												1.2%		1.2%
3.5								0.5%		0.5%	1.0%	1.7%		3.8%
3							0.5%	0.6%	0.5%	1.1%	1.4%	1.9%		6.2%
2.5						0.6%	1.0%	1.3%	1.2%	2.1%	2.9%	2.8%		11.9%
2				0.5%	1.3%	1.3%	1.4%	2.7%	2.3%	3.7%	3.8%	2.2%		19.2%
1.5			0.6%	1.7%	2.2%	1.4%	2.6%	6.5%	4.7%	5.0%	2.9%	1.2%		28.8%
1		0.6%	2.3%	2.1%	1.5%	1.8%	4.1%	6.6%	3.4%	2.2%	1.0%	0.9%		26.4%
0.5							0.8%	1.2%						1.9%
Total	0.0%	0.6%	2.9%	4.3%	5.0%	5.2%	10.4%	19.5%	12.0%	14.5%	13.0%	12.6%	0.0%	100.0%

Fig. 2. Occurrence of selected fatigue sea states (Hs-Tp combination)

Hs [m] (top of the bin) \ Tp [s] (top of the bin)	3	4	5	6	7	8	9	10	11	12	14	17	>17	Avg
>6														0.00
6														0.00
5.5														0.00
5														0.00
4.5												0.26		0.26
4												0.29		0.29
3.5								0.35		0.31	0.25	0.21		0.28
3							0.30	0.32	0.31	0.26	0.21	0.17		0.26
2.5						0.24	0.27	0.29	0.22	0.21	0.18	0.16		0.22
2				0.20	0.20	0.19	0.24	0.23	0.19	0.18	0.15	0.16		0.19
1.5			0.16	0.17	0.18	0.18	0.18	0.16	0.15	0.15	0.15	0.15		0.16
1		0.13	0.14	0.17	0.15	0.14	0.14	0.14	0.14	0.13	0.13	0.16		0.14
0.5							0.14	0.12						0.13
Avg	0.00	0.13	0.15	0.18	0.18	0.19	0.21	0.23	0.20	0.21	0.18	0.20	0.00	

Fig. 3. Average current associated with selected fatigue sea states (in m/s). Each combination of Tp-Hs represents a load case.

(315° from True North, TN). The probability of occurrence for each wave was then scaled up to account a total percentage occurrence of 100% for the selected sea states to ensure the total of the load cases cover a full year. The sea state combinations considered in the fatigue analysis are presented in Fig. 2.

The scatter diagram's mean current associated with each sea state is taken from [7], and the average current associated with the selected fatigue sea states is shown in Fig. 3. In this figure, the last column and last row show weighted averages.

Based on experience from previous projects, it is known that the wave conditions will largely influence the fatigue performance of the cable. On the other hand, the wind is unlikely to affect the results in the cable significantly as the buoy area exposed to the wind is very small. Hence, the wind is not influencing the dynamics of the buoy greatly and is not considered in the fatigue analysis.

The current was applied on each sea state, according to the averages given in Fig. 3. Since Eastward currents are prevalent on site, the current will be assumed to be coming from West (270° from TN). Each load case is represented by a combination of the wave height, wave period and the probability of that occurrence, taken from Fig. 3.

C. System Description

The HL2.0 is a cylindrical structure similar in shape to the Catenary Anchor Leg Mooring (CALM) buoy. It has three main structural elements, namely: hull, superstructure and inner (watertight) trunk; and three main spaces: (1) hold (2) trunk and (3) superstructure as presented in Fig. 4. The principal dimensions of HL2.0 are given in Table I.

The position of the Centre of Gravity (CoG) and the moments of inertia considered for the buoy are

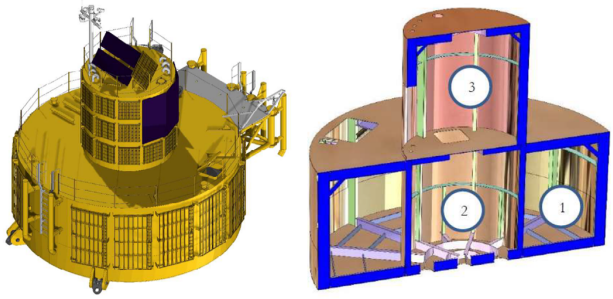

Fig. 4. Main structural elements and spaces of HarshLab 2.0.

TABLE I
PARTICULARS OF HARSHLAB 2.0

Component	Parameter	Value	Unit
Hull	Diameter	8.50	m
	Height	3.50	m
Housing	Diameter	3.50	m
	Height	3.50	m
Inner trunk	Diameter	3.50	m
	Height	3.50	m
Operating condition	Draft	2.44	m
	Displacement	141.77	te
	Mooring load	20.80	te

TABLE II
MASS AND INERTIA PROPERTIES OF HARSHLAB 2.0

Parameter		Value	Unit
Mass		120.970	te
Centre of Gravity	Longitudinal (LCG)	0.083	m
	Transverse (TCG)	0.013	m
	Vertical (VCG)	1.544	m
Moment of Inertia	Ixx	961.020	te.m^2
	Iyy	1331.930	te.m^2
	Izz	1544.320	te.m^2

summarised in Table II. It is noted that the CoG is slightly off-centre, leading to approximately $0.5°$ heeling and $2.8°$ trimming in equilibrium. The buoy operates at one loading condition with minor changes in the mass distribution due to the addition or removal of components to be tested.

The mooring system of the HL2.0 buoy is composed of three catenary mooring lines connected to the anchor points. Each mooring line combines 90 mm steel wire, 69 mm studless chain, and 76 mm studlink chain sections.

D. Cable

The dynamic cable is connected between the connector on the BiMEP cable and HL2.0. The selected cable is a double-armoured flexible cable with a relatively small weight in comparison to the outer diameter of the cross-section. The properties of the cable are listed in Table III.

TABLE III
DYNAMIC POWER CABLE PROPERTIES

Parameter	Value	Unit
Weight in air	7.23	kg/m
Weight in water	4.60	kg/m
Outer diameter	58.50	mm
Axial stiffness	110.74	MN
Flexural stiffness	0.24	kN.m^2
Torsional stiffness	4.19	kN.m^2
Maximum allowable load	125	kN
Minimum bend radius	705 (fixed) 880 (under tension)	mm

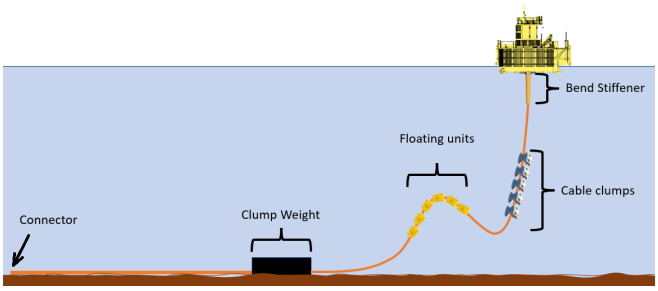

Fig. 5. Layout of the power cable showing the components added for protection and for the Lazy Wave configuration.

E. Design criteria

In the standard DNV-RP-F401, [8], it is specified that the safety factor on fatigue life for all the cable sections shall not be smaller than 10. Whilst this design target can be kept as an initial reference, lower safety factors can be accepted on specific cases when previously agreed [8]. Nonetheless, for this case study, the safety factor of 10 has been considered, giving a total of 100 years for the DPC fatigue life.

III. COMPUTATIONAL SETUP AND ANALYSIS

The fatigue analysis is performed using OrcaFlex. This software is based on the finite element method considering a lumped mass approach, where the line properties are assigned to nodes. Furthermore, it provides a fast and accurate analysis of a wide range of offshore systems under wave loads and externally imposed motions. The set of simulated load cases lasts 30 minutes, the minimum simulation time recommended by common industry standards when performing fatigue analysis, such as [9].

The layout of the power cable is presented in Fig. 5, where each of the components are shown. The ballast is given by cable clumps and the buoyancy by net-buoyancy floating units; these components contribute to the Lazy Wave configuration given to the cable. Additionally, the clump weight fixes the line at a location on the seabed to improve the stability of the cable and maintain the correct reference for the vertical plane of the cable.

Five DPC layouts are considered in the analysis. The first, identified as the *original* design, comprises a set of fourteen 120 kg cable clumps and ten 20 kg buoyancy modules. This layout is the preliminary design,

which is the outcome of several design iterations and considerations based on the most critical conditions at the operation site. During these iterations, the buoy model was calibrated against experimental tests using the Response Amplitude Operators (RAO), and the cable components' influence was examined. Nonetheless, despite using this model from [10], the scope of the present study on fatigue life does not cover the outcome details of the model building and components selection at the preliminary stage.

The additional models were proposed as part of a solution to increase the design life of the DPC, with slight modifications to the cable configuration from the original design. The details of the layouts considered are presented in Section IV-B.

A. Fatigue analysis overview

In principle, the fatigue life is estimated by comparing the long-term cyclic loading in each cable component with the resistance of that component to damage. First, the tension and moment calculated at specific power cable locations are obtained. Then, the stress range cycles are calculated. A cycle counting method separates the contribution of different constant-amplitude stress ranges (e.g. the rainflow method is widely used for time-domain simulations with irregular waves).

Following, the damage per stress range cycle, S_i, contributing to the failure is calculated, $D_i = 1/N_i$, and then the total damage is determined assuming the Palmgren-Miner rule, $D = \sum_{i=1}^{k} \frac{n_i}{N_i}$;the component will fail when D reaches unity, [4]. More specifically, the n_i is the number of cycles for the stress range S_i and N_i is taken from the $S-N$ curve of the material as the number of cycles to failure for the stress range S_i. The process is summarised in Fig. 6.

These damage values are calculated based on a year of exposure, using the probability of occurrence and presented as D_{year}. Finally, the fatigue life, L_f, and the design fatigue life, L_{fd}, are estimated using (1) and (2), respectively.

$$L_f = \frac{1}{D_{year}} \tag{1}$$

$$L_{f_d} = \frac{L_f}{SF} \tag{2}$$

SF is the safety factor based on the criteria for evaluating the design fatigue life, which is defined at ten for this study.

For the DPC, the damage for each variable was derived from $S-N$ and $\epsilon-N$ curves. In the following subsections, the methods used to estimate the fatigue life of the DPC are further detailed.

B. Stress - number of cycles ($\sigma - N$) method

For flexible risers and umbilicals, multiple components (layers) are subjected to fatigue; furthermore, there are material and geometric non-linearities. In this case, the localised stress is calculated as a function of the tension and curvature, see (3):

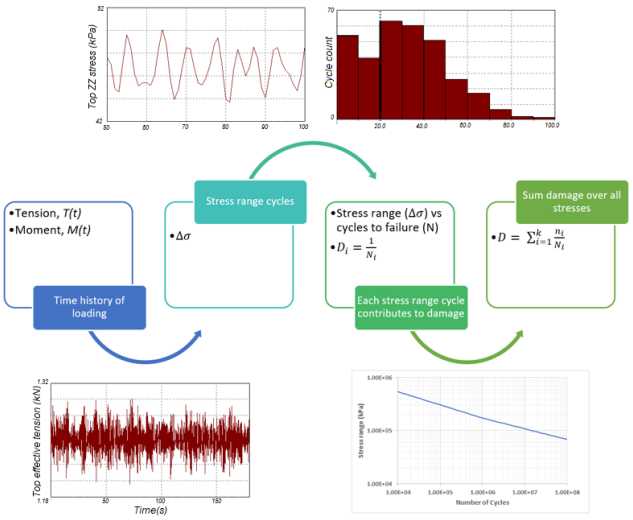

Fig. 6. Fatigue basics – calculation of total damage, D.

$$\sigma = K_t T + K_c(\theta, C) \tag{3}$$

where K_t is the tension stress factor, T is the wall tension (T_w) or the effective tension (T_e), K_c is the curvature stress factor as a function of θ, the radial position, and C, the pipe curvature. The wall tension, T_w, considers the effective tension, T_e, plus the contribution of the external and internal pressures. In the case of cables, the effect from the external pressure is expected to be negligible, whilst there is no internal pressure to be considered; this is further investigated and confirmed in the results section. Hence, the effective tension is used for the fatigue analyses of the cable components.

Additionally, the combined stresses accounting for the tension and bending stresses (the latter, at full slip stage) for the armour and the conductor are given in (4) and (5).

$$\sigma_{armour} = \frac{T}{A_{armour}} + E_{armour}\chi\frac{d_w}{2} \tag{4}$$

$$\sigma_{conductor} = E_{Cu}\frac{T}{E_{armour}A_{armour}} + E_{Cu}\chi\frac{d_c}{2} \tag{5}$$

In these equations, A_{armour} is the armour cross-sectional area, E is the high-strength steel Young's modulus, E_{Cu} is the copper Young's modulus, χ is the radius of curvature, d_w is the wire diameter and d_c is the conductor diameter. The expressions $d_w/2$ and $d_c/2$ are the radial positions of the outer components. Combining the localised stress equation with the ones for each specific layer, the tension stress factor for the outer layer of the wires is taken as $1/A_{armour}$ and the curvature stress factor as $E(d_w/2)$. Similarly, it is done for the conductor using $\sigma_{conductor}$. It is worth noting that these equations assume that the armour supports the full axial load.

The values obtained for the armour (high-strength steel) and the conductor (copper) for the stress-based analyses are summarised in Table IV.

TABLE IV
CHARACTERISTICS AND COEFFICIENTS OF THE ARMOUR AND THE CONDUCTOR

Parameter	Value	Unit
A_{armour}	5.55e-4	m^2
E_{armour}	2.10e8	kPa
E_{Cu}	2.10e8	kPa
d_w	2.50e-3	m
d_c	7.98e-3	m
$K_{t,armour}$	1802.82	kPa/kN
$K_{c,armour}$	2.63e5	kPa/(rad/m)
$K_{t,copper}$	987.26	kPa/kN
$K_{c,copper}$	4.59e5	kPa/(rad/m)

TABLE V
S-N CURVE PARAMETERS (STRESS UNITS: KPA)

Comp.	Low-cycle region N cycles		Region boundary, N (cycles)	High-cycle region N cycles	
	m_1	$\log a_1$		m_2	$\log a_2$
Armour	4.00	26.92	1e6	5.0	32.15
Conduct.	6.24	38.50	Infinity	-	-

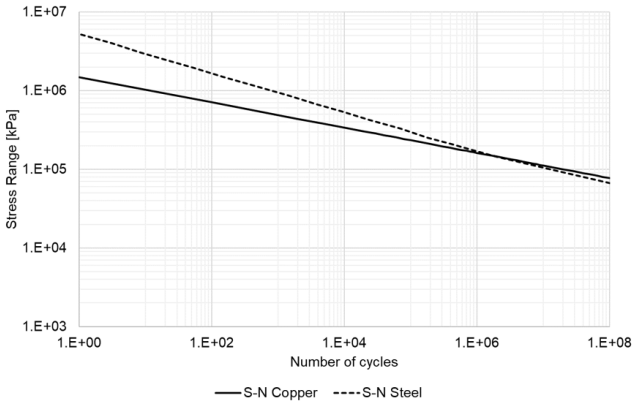

Fig. 7. $\sigma - N$ curves for the armour (high-strength steel, [4] and the conductor (copper), [11].

For both DPC components, armour and conductor, the $S-N$ curves are based on the parameters presented in Table V and using (6) to estimate the stress range, S:

$$N = aS^{-m} \tag{6}$$

where N is the number of cycles to failure, m and a are empirical constants fitted to test data. Once this is done for all the cases, the annual damage, fatigue life and design fatigue life are calculated.

The damage calculation uses the effective tension obtained from the OrcaFlex simulations and is estimated using an in-house script implemented using the methodology described in this section. The fatigue analysis is done within the software for the 51 load cases considered for the armour of the dynamic cable. The simulation period is 1800 s, and the exposure time is the total time the system is exposed to this load case, which covers the year using the probability

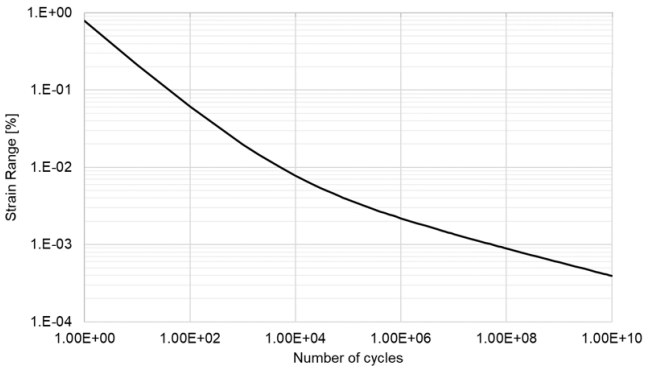

Fig. 8. $\epsilon - N$ curve for the copper; data retrieved from [12].

values. The least probable cases cover 47 hours at each case condition, whereas the most probable case (H_s = 0.75 m and T_p = 9.5 s) covers 579 hours during the year. The critical damage is set at a point of 0.1, and the number of points around the cable circumference is 16. These represent different angular positions on the cross-section plane and are referred to as *thetas*.

C. Strain - number of cycles ($\epsilon - N$) method

Another way to assess the fatigue of dynamic cables is using the strain-cycles, $\epsilon - N$; it is expected that this method is suitable as it considers the non-linear stress-strain effects resulting from the plastic strain, relevant when considering electrical cables (in this case, copper), [5], [12]. The tension and curvature strain factors equations are shown in (7) and (8), which consider the axial strain given by the armour and full slip. The strain-based tension factor is 8.585e-6 kN^{-1}, and the strain-based tension coefficient is 3.99e-3 m.

$$\epsilon = K_t T + K_c(\theta, C) \tag{7}$$

$$\epsilon = \frac{T}{E_{armour} A_{armour}} + \chi \frac{d_c}{2} \tag{8}$$

Similarly to the stress-based approach, the first step includes simulating the buoy, moorings and power cable according to the sea states that represent the conditions in the area of operation. Secondly, the values of the effective tension along the cable are taken from the simulations. The rainflow counting method is employed to account for the cycles per year corresponding to each strain range. The cycle counting method simplifies the complex strain (or stress) spectra into a series of cycles at an equal range.

In addition, this data is used to calculate the fatigue life using the strain-cycles curve of copper, shown in Fig 8. The values with a strain range below 1% (0.01) are expected to be in the elastic region.

IV. FATIGUE LIFE ESTIMATION

A. Preliminary design model

The preliminary design's fatigue life was estimated using the methods described previously. Among the results, it is found that there is excessive damage, over 0.1, for the conductor (stress-based approach), in a

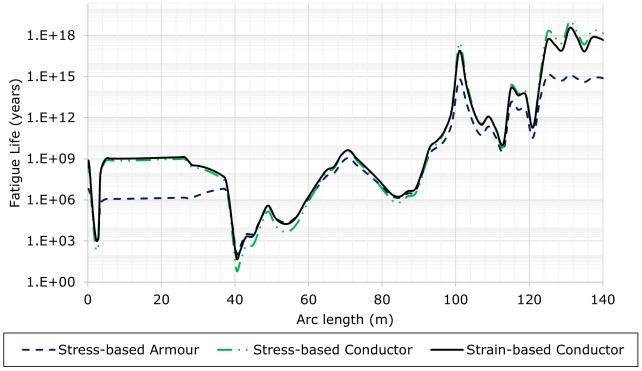

Fig. 9. Original model: fatigue life in years of the power cable considering the different segments and cable components.

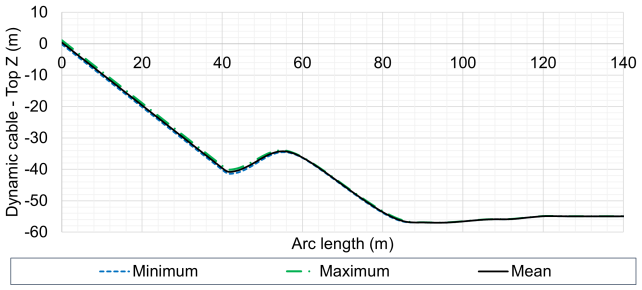

Fig. 10. Original model: motion of the cable in the z-direction during the simulation against the length of the cable (case: FLS-010).

range of 0.11 and 0.14. Consequently, the most critical section is located at 40.4 m, measured from the buoy at different points on the cable's circumference. This point belongs to the transition zone between clumps and floaters, which is subjected to the largest curvatures by the nature of the layout. This section's lowest estimated fatigue life is seven years; see Fig. 9.

Additionally, Fig. 9 shows that the stress- and strain-based conductor curves differ significantly at the critical locations, namely, the sections of the bend stiffener and between the cable clumps and floaters. The vertical outline of the power cable is shown in Fig. 10, indicating that the most critical point is aligned to the most vulnerable section of the cable due to its curvature contributing to the bending loads. Furthermore, the overall damage over the total exposure at the different key sections of the cable, along with the fatigue life estimated, is shown in Table VI.

The results shown in Fig. 9 coincide with the findings of the excessive damage values shown in Table IV-A, being the most critical at a location of 40.4 m from the buoy, where the low value of fatigue life is seen. The fatigue lives of the remaining cable segments tend to exceptionally large values since the damage is close to zero.

Fig. 11 shows the fatigue life curves estimated when using the effective and wall tensions. The difference between these two sets of curves is negligible for each of the methods used. Hence, for this particular case the fatigue life is estimated using the effective tension.

The design fatigue life of one year does not comply with the design criteria of the project's life, which is ten years. Hence, additional models with slight

TABLE VI
ORIGINAL MODEL: RANGE OF EXCESSIVE DAMAGE IN THE FATIGUE ANALYSIS USING THE EFFECTIVE TENSION AND THE RAINFLOW COUNTING METHOD

Arclength (m)	Method	Overall damage over total exposure, D_{year}	Life (years), L_f	Design fatigue life, L_{fd}
2.125		0.00306	327	33
2.375		0.00503	199	20
2.625	Conductor	0.00376	266	27
40.43	stress-based	0.14269	7	1
41.44		0.03023	33	3
42.95		0.00241	415	42

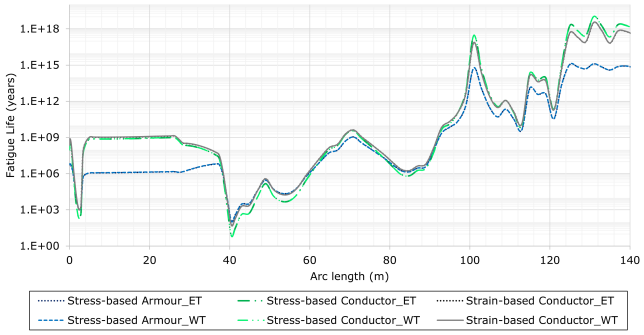

Fig. 11. Fatigue life predicted using the effective tension, ET, and the wall tension, WT.

modifications from the preliminary design were examined in the next subsection. These minor modifications comprise changes in the layout and the components' specifications.

B. Layout analysis

The preliminary model analysed previously resulted from several design iterations and considerations undertaken at the initial stage. Further models were assessed based on the short fatigue life encountered, particularly in the region between the cable clumps and floaters. These modifications allow more flexibility in the affected section without significantly compromising the cable response at the section where the bend stiffener is located. Moreover, different buoyancy and ballast capacities were investigated to provide a range of suitable components for a later procurement stage. Table VII lists the layouts considered during this study.

The estimated fatigue life values for the models described in Table VII are presented in Fig. 12. The values in this figure are based on the worst component measured when considering the stress- or strain-based methods. As a result, these values are considerably more conservative. The modified models all tend to have fatigue failure at the same cable sections, at the bend stiffener or between the ballast and buoyancy modules. The deviations throughout the cable where the fatigue life estimates are exceptionally large are not

TABLE VII
MAIN PARTICULARS OF THE DIFFERENT MODELS OF CABLE CONFIGURATIONS

Case	Description	Cable clumps	Floating units
1	Preliminary design, original	14 x 120 kg	10 x 20 kg
2	Modif. model 1	12 x 120 kg	10 x 20 kg
3	Modif. model 2	14 x 120 kg (shifted location)	10 x 20 kg
4	Modif. model 3	14 x 120 kg (shifted location)	12 x 15 kg (shifted location)
5	Modif. model 4	14 x 85 kg (shifted location)	12 x 18 kg (shifted location)

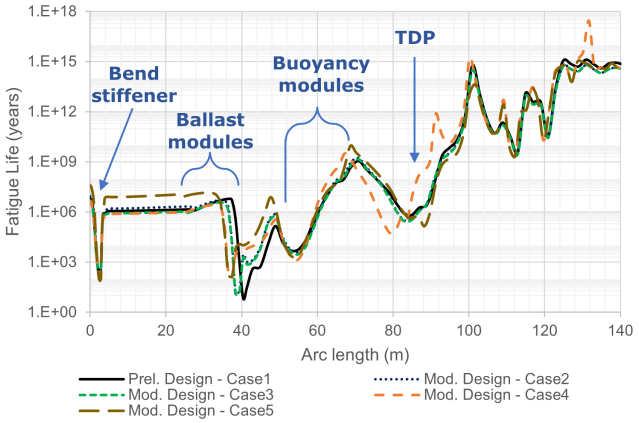

Fig. 12. Fatigue life in years of the power cable considering slight modifications in the layout and its components.

of interest since these comply with the design criteria defined.

The alterations undertaken in the model negatively affect the fatigue life at the section where the bend stiffener is located; see Fig. 13. Whereas in the section between the cable clumps and the floating units, the fatigue life in the modified models is improved against the preliminary design, see Fig. 14. This suggests the presence of a trade-off between satisfactory fatigue performance in these two cable sections (bend stiffener and clump-float transition zone).

Regarding complying with the design criteria, it seems that the model *Case4*, is the only layout that ensures a fatigue life of over 100 years across the whole arc length; see Table VIII. In general, the behaviour across the length of the DPC is similar between the different approaches, leading to a reduced fatigue life on the locations near the bend stiffener and the belly (sagbend) of the cable (between the clump weights and the floaters).

Overall, the modified models' fatigue life is enhanced, increasing from a minimum of 7 years to a minimum of 109 years for the modified design, *Case4*. Notably, the fatigue life in the section near the bend stiffener has been reduced by these changes (from 199 to 144 years). However, the minimum fatigue life in the bend stiffener region is still well within the design criteria. In Fig. 15, the worst component failure along the cable of *Case4* is shown. In this case, the methods

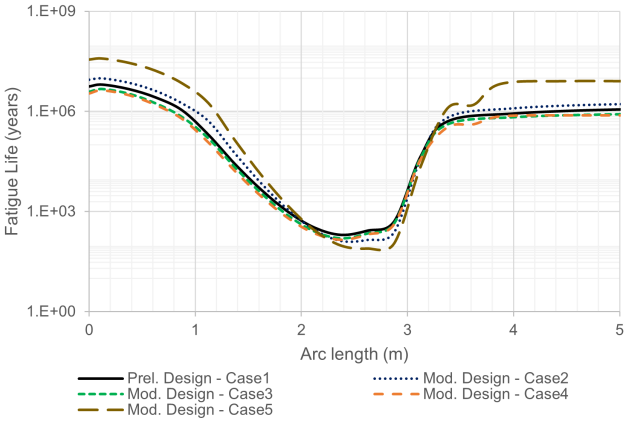

Fig. 13. Cable fatigue life at the bend stiffener section when considering slight modifications in the layout and its components.

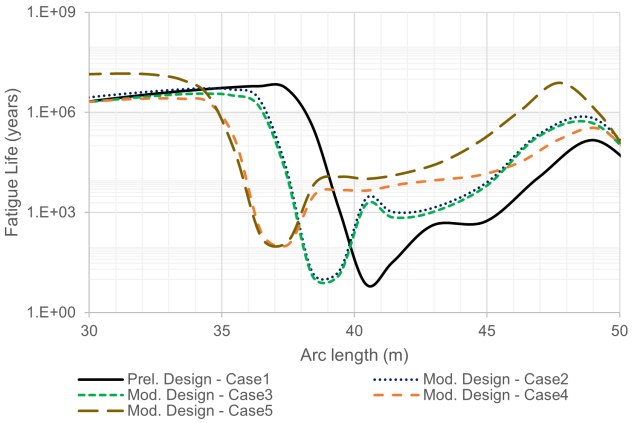

Fig. 14. Cable fatigue life at section between the ballast and buoyancy modules when considering slight modifications in the layout and its components.

TABLE VIII
FATIGUE LIFE ASSESSED FOR ALL THE MODELS, ORIGINAL AND MODIFIED DESIGNS, AT DIFFERENT CABLE LOCATIONS (YEARS)

Arclength (m)	L_f, Case1	L_f, Case2	L_f, Case3	L_f, Case4	L_f, Case5
2.125	327	279	254	224	273
2.375	199	131	158	144	95
2.625	266	140	221	208	78
2.875	>500	238	442	423	111
37.500	>500	>500	>500	109	141
38.410	>500	16	13	>500	>500
39.420	>500	18	14	>500	>500
40.430	7	>500	>500	>500	>500
41.440	33	>500	>500	>500	>500
42.950	415	>500	>500	>500	>500

failing are using the stress-based approach for the armour (A.F.) and the conductor (C.F.). It is worth noting that the current stress and strain calculation does not account for the lay angles in the armour and copper wires. This further sophistication may contribute to reducing fatigue damage (stresses would decrease due to a larger tensile area).

In the case of the conductor, the stress and strain curves are based on tests undertaken considering a

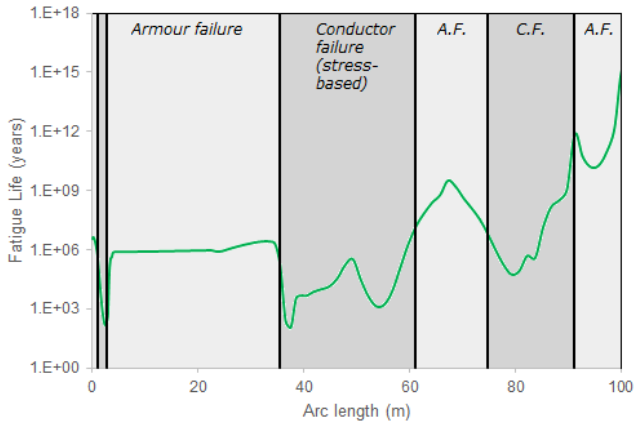

Fig. 15. Modified design Case4: fatigue life estimated and the worst component failure measured along the cable.

95 mm^2 copper conductor of similar characteristics, retrieved from [11] and [12], respectively. However, in the case of the $\sigma - N$ curve, the values used are based on the nominal stress (without the bending correction), which brings to more conservative values. For example, when using bending correction, the cable with the original design, *Case1*, will increase its minimum fatigue life to 9 years, which is a slight increase at a localised fault along the cable. In the case of the modified design, *Case2*, the fatigue life would increase to 20 years when using the stress-based approach (for the conductor).

V. Conclusion

This paper has presented the results from the design and engineering of a dynamic power cable for the HarshLab testing facility, focusing on its fatigue performance. Dynamic power cables are a key component to enable the future exploitation of offshore renewable energies. However, their development and implementation are challenged by their reliability and fatigue life, and the design of the subsea cable configuration needs to consider these aspects early on.

Performing detailed time-domain dynamic analysis to evaluate the fatigue performance of subsea cables has been shown essential to carry out the fatigue analysis to the appropriate level of detail. Considering the approaches available in the literature, fatigue in cables can be determined reliably by carrying out a rainflow-cycle analysis of the time series for the relevant stresses and strains in the cable cross-section.

An extensive review has been carried out on the range of methods and approaches found in the literature for the fatigue assessment of dynamic cables, and appropriate $S - N$ and $\epsilon - N$ curves for the analysis were established.

The fatigue life of a power cable has been assessed using stress- and strain-based approaches for its armour and conductor core (copper wire), considering five different cable layouts with variations in the ballast and buoyancy units. The first model considered a preliminary design, whereas the additional models were proposed as part of a solution to increase the design life of the DPC, with minor modifications to the cable configuration.

Analysis of the preliminary design showed that the cable is prone to fatigue damage, leading to a fatigue life of only 7 years in the worst case. The sections in the cable most sensitive to poor fatigue performance were found to correspond with the sag-bend region (in the transition between clumps and floats) and close to the hang-off point at the buoy, where the stiffener is located.

Results for the other configurations have shown that the fatigue performance is severely affected by the configuration of the cable layout, and even slight changes in the position and definition of the ancillary elements used in the layout (e.g. floats, clumps, stiffener) have a dramatic impact on the fatigue response of the cable.

An optimisation of the cable layout was therefore performed by introducing slight changes in the type and position of the clumps and floats. The optimised configuration led to a significant improvement in the fatigue life with a minimum design life exceeding the target of 10 years.

In conclusion, a slight change to the cable configuration design gives more flexibility to the section between the clumps and the floaters, improving its fatigue life considerably at the expense of the section of the bend stiffener. Furthermore, it is found that despite the value deviations found in the methods applied, this approach is fairly conservative, leading to a satisfactory DPC fatigue life.

Even though the final results were satisfactory for proceeding with the procurement of cable and finalisation of the design, this work has identified several aspects that may need further investigation in the future.

The stress and strain models currently being applied to analyse dynamic cable assume an even distribution of the loads and stresses. More sophisticated analysis involving FE modelling may be performed in later stages. However, the results were corroborated by the approaches applied in the literature.

The authors have found that there is limited guidance from existing industry standards on expected fatigue life safety factors and fatigue performance of dynamic cables for offshore renewable applications. There does not seem to be a recognised and standardised approach to perform fatigue testing of cable and the development of limit $S - N$ curves has been based on previous literature with very little consideration of the specific cable cross-section considered here. Future steps in the project will include the engagement with the cable manufacturer to ensure that the right limitation for the fatigue responses are considered and that potential testing programs are undertaken to validate these results.

References

[1] P. R. Thies, L. Johanning, and G. H. Smith, "Assessing mechanical loading regimes and fatigue life of marine power cables in marine energy applications," vol. 226, 2 2012, pp. 18–32.
[2] CORES, "D3.05 – specifications of power umbilical components," 2009.

[3] F. P. Nasution, S. Sævik, and J. K. Gjøsteen, "Finite element analysis of the fatigue strength of copper power conductors exposed to tension and bending loads," *International Journal of Fatigue*, vol. 59, pp. 114–128, 2014.
[4] DNV-GL, "Rp-c203: Fatigue design of offshore steel structures," 6 2014. [Online]. Available: www.dnvgl.com.
[5] M. Sobhaniasl, F. Petrini, M. Karimirad, and F. Bontempi, "Fatigue life assessment for power cables in floating offshorewind turbines," *Energies*, vol. 13, 6 2020.
[6] Tecnalia, "Harshlab: el mayor laboratorio flotante para la industria offshore," 9 2022. [Online]. Available: https://harshlab.eu/2022/09/harshlab-el-mayor-laboratorio-flotante-para-la-industria-offshore/
[7] TRLPlus, "Metocean analysis of bimep for offshore design," 3 2017.
[8] DNV-GL, "Dnv-rp-f401: Electrical power cables in subsea applications," 2017. [Online]. Available: http://www.dnvgl.com,
[9] B. Veritas, "Rule note nr 493 dt r04 e: Classification of mooring systems for permanent and mobile offshore units," 2021.
[10] T. Limited, "Basis of dynamic cable design," 2022.
[11] F. P. Nasution, S. Sævik, and J. K. Gjøsteen, "Fatigue analysis of copper conductor for offshore wind turbines by experimental and fe method," vol. 24. Elsevier Ltd, 2012, pp. 271–280.
[12] S. Karlsen, R. Slora, K. Heide, S. Lund, F. Eggertsen, and P. A. Osborg, "Dynamic deep water power cables," 2009, pp. 15–18.